



## Measurement report: Variations in surface SO<sub>2</sub> and NO<sub>x</sub> mixing ratios from 2004 to 2016 at a background site in the North China Plain

Xueli Liu<sup>1</sup>, Liang Ran<sup>2</sup>, Weili Lin<sup>1\*</sup>, Xiaobin Xu<sup>3</sup>, Zhiqiang Ma<sup>4</sup>, Fan Dong<sup>4</sup>, Di He<sup>4</sup>, Liyan Zhou<sup>4</sup>, Qingfeng Shi<sup>4</sup>, and Yao Wang<sup>4</sup>

<sup>1</sup>Key Laboratory of Ecology and Environment in Minority Areas (Minzu University of China), National Ethnic Affairs Commission, Beijing 100081, China

<sup>2</sup>Key Laboratory of Middle Atmosphere and Global Environment Observation, Institute of Atmospheric Physics, Chinese Academy of Sciences, Beijing, 100089, China

<sup>3</sup>Chinese Academy of Meteorological Sciences, Beijing, 100081, China

<sup>4</sup>Beijing Shangdianzi Regional Atmosphere Watch Station, Beijing, 101507, China

*Correspondence to:* Weili Lin (linwl@muc.edu.cn)

1 **Abstract.** Strict air pollution control strategies have been implemented in recent decades in the North China Plain  
2 (NCP), previously one of the most polluted regions in the world, and have resulted in considerable changes in  
3 emissions of air pollutants. However, little is so far known about the long-term trends of the regional background  
4 level of NO<sub>x</sub> and SO<sub>2</sub>, along with the increase and decrease processes of regional emissions. In this study, the  
5 seasonal and diurnal variations of NO<sub>x</sub> and SO<sub>2</sub> as well as their long-term trends at a regional background station in  
6 the NCP were characterized from 2004 to 2016. On average, SO<sub>2</sub> and NO<sub>x</sub> mixing ratios were  $5.7 \pm 8.4$  ppb and  
7  $14.2 \pm 12.4$  ppb, respectively. The seasonal variations in SO<sub>2</sub> and NO<sub>x</sub> mixing ratios showed a similar pattern with a  
8 peak in winter and a valley in summer. However, the diurnal variations in SO<sub>2</sub> and NO<sub>x</sub> mixing ratios greatly  
9 differed for all seasons, indicating different sources for SO<sub>2</sub> and NO<sub>x</sub>. Overall, the annual mean SO<sub>2</sub> exhibited a  
10 significant decreasing trend of  $-6.1 \text{ \% yr}^{-1}$  ( $R = -0.84$ ,  $P < 0.01$ ) from 2004 to 2016, which is very close to  $-6.3 \text{ \%}$   
11  $\text{yr}^{-1}$  of the annual SO<sub>2</sub> emission in Beijing, and a greater decreasing trend of  $-7.4 \text{ \% yr}^{-1}$  ( $R = -0.95$ ,  $P < 0.01$ ) from  
12 2008 to 2016. The annual mean of NO<sub>x</sub> showed a fluctuating rise of  $+3.4 \text{ \% yr}^{-1}$  ( $R = 0.38$ ,  $P = 0.40$ ) from 2005 to  
13 2010, reaching the peak value (16.9 ppb) in 2010, and then exhibited an extremely significant fluctuating downward  
14 trend of  $-4.5 \text{ \% yr}^{-1}$  ( $R = 0.95$ ,  $P < 0.01$ ) from 2010 to 2016. After 2010, the annual mean NO<sub>x</sub> mixing ratios  
15 correlated significantly ( $R = 0.94$ ,  $P < 0.01$ ) with the annual NO<sub>x</sub> emission in North China. The decreasing rate  
16 ( $-4.8 \text{ \% yr}^{-1}$ ,  $R = -0.92$ ,  $P < 0.01$ ) of the annual mean NO<sub>x</sub> mixing ratios from 2011 to 2016 at SDZ are lower than  
17 the one ( $-8.8 \text{ \% yr}^{-1}$ ,  $R = -0.94$ ,  $P < 0.01$ ) for the annual NO<sub>x</sub> emission in the NCP and ( $-9.0 \text{ \% yr}^{-1}$ ,  $R = -0.96$ ,  $P <$   
18  $0.01$ ) in Beijing. It indicated that surface NO<sub>x</sub> mixing ratios at SDZ had weaker influence than SO<sub>2</sub> by the emission



19 reduction in Beijing and its surrounding areas in the NCP. The increase in the amount of motor vehicles led to an  
20 increase in traffic emissions for  $\text{NO}_x$ . This study supported conclusions from previous studies that the measures  
21 taken for controlling  $\text{NO}_x$  and  $\text{SO}_2$  in the NCP in the past decades were generally successful. However,  $\text{NO}_x$   
22 emission control should be strengthened in the future.

## 23 **1 Introduction**

24 Acid gases sulfur dioxide ( $\text{SO}_2$ ) and nitrogen oxides ( $\text{NO}_x$ ) are closely related to climate, ecology, environment and  
25 human health. They are important gaseous pollutants in China (Xu et al., 2009) and also recommended by the  
26 Global Atmosphere Watch (GAW) of the World Meteorological Organization (WMO) for priority observation  
27 (WMO, 2001). They can also be transformed into nitrate and sulfate aerosols, which play an important role in the  
28 formation of aerosol pollution and acid rain (Yang et al., 2011; Cheng et al., 2013; Luo et al., 2016; Chen et al.,  
29 2017). Sulfate and nitrate constitute more than 1/3 of  $\text{PM}_{2.5}$  mass concentration and can cause serious respiratory  
30 diseases (Yang et al., 2010; Yang et al., 2011; Gao et al., 2012; Zhao et al., 2013; Liu et al., 2014).

31 With the economic development, population growth and rapid urbanization, air pollution in China exhibited the  
32 characteristics of regional pollution centering urban areas in recent years (Shao et al., 2006; Xu et al., 2008). Many  
33 studies thereby focused on regional pollution (Qi et al., 2012; Li et al., 2015), instead of local and suburban  
34 pollution as previously did (Liu et al., 2008; Lin et al., 2009). The North China Plain (NCP), a heavily industrialized  
35 and densely populated area with considerable agricultural activities, is one of the most polluted regions of the world.  
36 The strong emissions of  $\text{SO}_2$  and  $\text{NO}_x$  in the NCP showed the typical regional characteristics (Wu et al., 2010; Lin et  
37 al., 2012; Liu et al., 2014). Previous studies have combined observations at the background site and the urban site  
38 for comparisons (Liu et al., 2014), or selected short-term observations (1–2 years or 1–2 seasons) for the  
39 comparative study before and after major activities, in order to quantitatively evaluate the effect of implementing  
40 control measures during the event (Cheng et al., 2015; Li et al., 2019; Lin et al., 2011; Lin et al., 2012; Wei et al.,  
41 2016; Wu et al., 2010; Zhong et al., 2020). Most of the long-term studies (more than 10 years) evaluated the  
42 temporal and spatial variations of  $\text{SO}_2$  and  $\text{NO}_x$  based on satellite measurements of the vertical column density  
43 (Zhang et al., 2007; Cai et al., 2018; Shikwambana et al., 2020). However, there were few studies on the long-term  
44 trend of  $\text{SO}_2$  and  $\text{NO}_x$  based on ground-level observations, especially in the background area of the NCP and with a  
45 time span of more than 10 years.



46 In this study, we analyzed the long-term variations in surface SO<sub>2</sub> and NO<sub>x</sub> mixing ratios observed at a regional  
47 WMO GAW station in the NCP, and discussed their influencing factors and their responses to pollution control  
48 measures, so as to provide scientific basis for designing further strategies for controlling SO<sub>2</sub> and NO<sub>x</sub> on a regional  
49 scale.

## 50 **2 Data and methods**

51 Surface SO<sub>2</sub> and NO<sub>x</sub> mixing ratios were measured at the Shangdianzi (SDZ) regional atmospheric background  
52 station (117°07' E, 40°39' N, 293.3 m a.s.l.). SDZ is located in Shangdianzi Village in Miyun District of Beijing,  
53 China. It is about 110 km northeast of urban Beijing. The measurements of air pollutants at this site could represent  
54 the background conditions in the NCP (Lin et al., 2008; Meng et al., 2009).

55 SDZ is situated on the north hill side of a northeast-to-southwest valley, with farmlands in the south. Corn and  
56 wheat were the main crops, but were recently replaced by fruit trees. It lies in a warm temperate and semi-humid  
57 climate zone, with short spring and autumn but long winter and summer. The monthly averages of meteorological  
58 parameters such as temperature (T), pressure (P), precipitation (PRCP), relative humidity (RH), wind speed (WS)  
59 and wind direction are shown in Fig. 1. Precipitation occurs mainly in summer. The prevailing wind directions were  
60 from NE–ENE and WSW–SW. Stronger wind speeds appear in spring and weaker in summer.

61 In-situ measurements of SO<sub>2</sub> and NO<sub>x</sub> mixing ratios were made using a pulsed fluorescence SO<sub>2</sub> analyzer (Model  
62 43C-TL, Thermo Fisher Scientific, MA, USA) and a chemiluminescence NO<sub>x</sub> analyzer (Model 42C-TL, Thermo  
63 Fisher Scientific, MA, USA), respectively. The detection limits of the Model 43C-TL SO<sub>2</sub> analyzer and the Model  
64 42C-TL NO<sub>x</sub> analyzer are 0.05 ppb (300 second averaging time) and 0.05 ppb (120 second averaging time),  
65 respectively. The wind speed (WS), wind direction (WD), air temperature (T), precipitation (PRCP), relative  
66 humidity (RH), and atmospheric pressure (P) during the same period are from the routine meteorological  
67 observations. In order to obtain long-term trends of atmospheric components at a regional atmospheric background  
68 station, the observations are required to be accurate, reliable, and comparable. Therefore, strict and effective quality  
69 control measures were implemented during the observation (Lin et al., 2009). Daily zero and span checks were  
70 routinely and automatically carried out. Multi-point calibrations were done monthly. The standard gases used at the  
71 site were compared against NIST-traceable standard gases to ensure the data comparability (Lin et al., 2009). During  
72 the period from January 2005 to May 2017, the percentages of effective hourly mean data of SO<sub>2</sub> and NO<sub>x</sub> are  
73 97.1 % and 96.7 %, respectively.



## 74 **3 Results**

### 75 **3.1 Observational levels**

76 The time series and statistic results of hourly mean SO<sub>2</sub> and NO<sub>x</sub> mixing ratios during the observational period at  
77 SDZ are showed in Fig. 2 and Table 1, respectively. The hourly mean SO<sub>2</sub> mixing ratios ranged from 0.01 to 100.34  
78 ppb, with 193 hours (0.18 %) exceeded the limit of 57 ppb set in China National Ambient Air Quality Standard  
79 (GB3095–2012, Grade I). The hourly mean NO<sub>2</sub> mixing ratios ranged from 0.01 to 124.4 ppb, with 5 hours  
80 exceeding the limit of 106 ppb (GB3095–2012, Grade I). The SO<sub>2</sub> mixing ratios exhibited an extremely significant  
81 downward trend ( $-0.37 \text{ ppb yr}^{-1}$ ,  $R = -0.20$ ,  $P < 0.01$ ) during the measurement period and a higher downward trend  
82 ( $-1.10 \text{ ppb yr}^{-1}$ ,  $R = -0.22$ ,  $P < 0.01$ ) from 2013 to 2017. The NO<sub>x</sub> mixing ratios exhibited a much smaller but  
83 significant downward trend ( $-0.03 \text{ ppb yr}^{-1}$ ,  $R = -0.01$ ,  $P < 0.05$ ). Details in the trends and the influencing factors  
84 will be discussed in Sect. 3.4.

85 As shown in Table 1, the average values  $\pm 1\sigma$  (standard deviation) of SO<sub>2</sub>, NO, NO<sub>2</sub>, and NO<sub>x</sub> concentrations are 5.7  
86  $\pm 8.4$  ppb, 1.1  $\pm 2.6$  ppb, 13.1  $\pm 10.9$  ppb, and 14.2  $\pm 12.4$  ppb, respectively. The results were close to the annual  
87 average concentrations of SO<sub>2</sub> (5.9  $\pm 10.0$  ppb), NO (0.8  $\pm 2.0$  ppb), NO<sub>2</sub> (13.8  $\pm 13.1$  ppb), and NO<sub>x</sub> (14.5  $\pm 14.0$   
88 ppb) at SDZ in 2004 reported by Meng et al. (2009). Compared with other background stations in China (Table 2),  
89 the SO<sub>2</sub> and NO<sub>x</sub> mixing ratios at SDZ are both at a relatively high level.

### 90 **3.2 Monthly variations**

91 Surface SO<sub>2</sub> and NO<sub>x</sub> mixing ratios at SDZ showed a similar seasonal pattern with high value in winter and low in  
92 summer (Fig. 3). The highest SO<sub>2</sub> level appeared in winter (9.46 ppb) with the maximum monthly mean in February  
93 (10.57 ppb), followed by that in spring (7.28 ppb) and autumn (5.01 ppb), and the lowest in summer (2.06 ppb) with  
94 the minimum in July (1.45 ppb). The concentration of NO<sub>x</sub> was higher in winter (18.12 ppb) and autumn (16.51  
95 ppb), lower in spring (12.95 ppb) and summer (9.24 ppb). The maximum monthly mean NO<sub>x</sub> appeared in November  
96 (21.70 ppb) and the minimum one in August (8.69 ppb). The seasonal patterns of SO<sub>2</sub> and NO<sub>x</sub> at SDZ were similar  
97 to those in urban and rural areas in North China (Meng et al., 2009; Lin et al., 2012; Song et al., 2016; Tang et al.,  
98 2016; Chen, 2017; Zhao et al., 2020), which were characterized by high levels in the heating season and low levels  
99 in summer.

100 The heating season in North China was from November to March. The emissions of SO<sub>2</sub> and NO<sub>x</sub> in the heating  
101 season were higher than those in the non-heating seasons. Compared with the non-heating seasons, lower  
102 temperature, drier air, weaker solar radiation, less precipitation, and lower mixing depth height were found in the



103 heating season, resulting in lower atmospheric chemical reaction rate of SO<sub>2</sub> and NO<sub>x</sub>, smaller removal effect of  
104 precipitation, weaker vertical diffusion, longer atmospheric lifetime, and thus higher concentrations.

### 105 3.3 Diurnal variations

106 The average diurnal variations in SO<sub>2</sub> and NO<sub>x</sub> mixing ratios at SDZ in different seasons are shown in Fig. 4. The  
107 SO<sub>2</sub> mixing ratios peaked at 14:00 in spring, 11:00 in summer, 15:00 in fall, and 16:00 in winter. The NO<sub>x</sub> mixing  
108 ratios peaked at 2:00 in fall, 3:00 in summer and winter, and 6:00 in spring. In addition, the valley of SO<sub>2</sub> diurnal  
109 cycle appeared at 6:00 in spring, 5:00 in summer, 5:00 in fall, and 6:00 in winter, respectively, whereas for NO<sub>x</sub> it  
110 was at 12:00, 13:00, 13:00, and 12:00, respectively. The diurnal behaviors of NO<sub>x</sub> and SO<sub>2</sub> mixing ratios are  
111 different. Generally, the average daily amplitudes of SO<sub>2</sub> are 4.36 ppb in spring, 1.99 ppb in summer, 4.18 ppb in  
112 fall, and 3.48 ppb in winter, respectively, while the average daily amplitudes of NO<sub>x</sub> are 6.83 ppb in spring, 6.27 in  
113 summer, 10.64 ppb in fall and 10.35 ppb in winter, respectively.

### 114 3.4 Long-term trends of SO<sub>2</sub> and NO<sub>x</sub> mixing ratios

115 Figure 5a showed the annual mean SO<sub>2</sub> mixing ratios from 2004 to 2016 at SDZ site, as well as the annual SO<sub>2</sub>  
116 emissions in North China (including Beijing, Tianjin, Hebei, Shanxi and Inner Mongolia). The annual mean SO<sub>2</sub>  
117 mixing ratio in 2004 was from Meng et al. (2009). The SO<sub>2</sub> emission peaked in 2006 and then decreased with years.  
118 Meanwhile, the annual mean SO<sub>2</sub> mixing ratio reached a high level around 7.6 ppb during 2006-2008, and then  
119 began to decline thereafter. A rebound in SO<sub>2</sub> emission occurred in 2011, while a lagged rise of SO<sub>2</sub> mixing ratio  
120 occurred in 2012. Overall, the annual mean SO<sub>2</sub> exhibited a significant decreasing trend of  $-0.36 \text{ ppb yr}^{-1}$  ( $-6.1 \text{ \% yr}^{-1}$ ,  
121  $R = -0.84$ ,  $P < 0.01$ ) from 2004 to 2016 and a greater decreasing trend of  $-0.56 \text{ ppb yr}^{-1}$  ( $-7.4 \text{ \% yr}^{-1}$ ,  $R = -0.95$ ,  
122  $P < 0.01$ ) from 2008 to 2016.

123 Figure 5b showed the long-term variations in the annual 5th and 95th percentile values of the hourly mean SO<sub>2</sub> in  
124 different years. The 95th percentile indicated the influence of polluted air masses, while the 5th percentile indicated  
125 the influence of clean air masses. Similar to the trends of annual mean SO<sub>2</sub> mixing ratios, the 95th percentile of SO<sub>2</sub>  
126 reached its peak (30.87 ppb) in 2007, and a little decrease in 2008 (29.19 ppb). After 2008, it began to decline.  
127 Compared with the SO<sub>2</sub> level in 2008, there was a great decrease ( $-19.8 \text{ \%}$ ) in 2009, but from 2009 to 2012 there  
128 was no significant decline in annual mean of SO<sub>2</sub>. The most significant downward trend of the 95th percentile of  
129 SO<sub>2</sub> was found from 2012 to 2016 with a rate of  $-3.98 \text{ ppb yr}^{-1}$  ( $-16.3 \text{ \% yr}^{-1}$ ,  $R = -0.99$ ,  $P < 0.01$ ). However, the



130 5th percentile of SO<sub>2</sub> mixing ratios did not change significantly of  $-0.05 \text{ ppb yr}^{-1}$  ( $-2.6 \% \text{ yr}^{-1}$ ,  $R = -0.15$ ,  $P = 0.6$ )  
131 from 2005 to 2016.

132 The annual mean of NO<sub>x</sub> showed an increasing trend of  $+0.37 \text{ ppb yr}^{-1}$  ( $+3.4 \% \text{ yr}^{-1}$ ,  $R = 0.38$ ,  $P = 0.40$ ) from 2005  
133 to 2010 with strong fluctuations (Fig. 5c,d). The annual NO<sub>x</sub> mean reached the peak value (16.93 ppb) in 2010, and  
134 exhibited a significant downward trend of  $-0.77 \text{ ppb yr}^{-1}$  ( $-4.5 \% \text{ yr}^{-1}$ ,  $R = 0.95$ ,  $P < 0.01$ ) from 2010 to 2016 (Fig.  
135 5c). The 95th percentile of the hourly mean of NO<sub>x</sub> firstly increased during 2005–2012 with  $+0.02 \text{ ppb yr}^{-1}$  ( $+0.1 \%$   
136  $\text{yr}^{-1}$ ,  $R = 0.73$ ,  $P < 0.05$ ) and then decreased during 2012–2016 with  $-0.03 \text{ ppb yr}^{-1}$  ( $-4.7 \% \text{ yr}^{-1}$ ,  $R = 0.95$ ,  $P < 0.05$ ).  
137 Similar to SO<sub>2</sub>, the annual 5th percentile of NO<sub>x</sub> mixing ratios did not change significantly ( $-1.7 \% \text{ yr}^{-1}$ ,  $R = -0.18$ ,  
138  $P = 0.58$ ) from 2005–2016 (Fig. 5d).

139 We regrouped NO<sub>x</sub> and SO<sub>2</sub> data into 4 subsets according to the heating period (November–March), spring  
140 (April–May), summer (June–August), and autumn (September–October). The long-term trends of the four subsets  
141 are shown in Fig. 6. The SO<sub>2</sub> mixing ratios showed significant downward trends of  $-0.96 \text{ ppb yr}^{-1}$  ( $-8.0 \% \text{ yr}^{-1}$ ,  $R =$   
142  $-0.99$ ,  $P < 0.01$ ) in the heating period,  $-0.39 \text{ ppb yr}^{-1}$  ( $-5.2 \% \text{ yr}^{-1}$ ,  $R = -0.84$ ,  $P < 0.01$ ) in spring,  $-0.24 \text{ ppb yr}^{-1}$   
143 ( $-4.3 \% \text{ yr}^{-1}$ ,  $R = -0.92$ ,  $P < 0.01$ ) in autumn, and  $-0.18 \text{ ppb yr}^{-1}$  ( $-7.7 \% \text{ yr}^{-1}$ ,  $R = -0.87$ ,  $P < 0.01$ ) in summer. The  
144 large reduction in the SO<sub>2</sub> level in the heating season was largely related to burning natural gas instead of coal for  
145 domestic heating (Qiu et al., 2017; Li et al., 2020).

146 Except for autumn, the trends of the annual mean NO<sub>x</sub> mixing ratios in other seasons showed a similar pattern that  
147 NO<sub>x</sub> mixing ratio rose firstly and then declined significantly. The annual mean of NO<sub>x</sub> in autumn showed a  
148 downward but statistically insignificant trend of  $-0.08 \text{ ppb yr}^{-1}$  ( $-0.6 \% \text{ yr}^{-1}$ ,  $R = -0.28$ ,  $P = 0.38$ ) from 2005 to  
149 2016. In other seasons, the peaks of NO<sub>x</sub> appeared in different years. The NO<sub>x</sub> mixing ratios showed significant  
150 downward trends of  $-1.16 \text{ ppb yr}^{-1}$  ( $-5.4 \% \text{ yr}^{-1}$ ,  $R = -0.84$ ,  $P < 0.05$ ) in the heating period during 2012–2016,  $-1.07$   
151  $\text{ppb yr}^{-1}$  ( $-7.6 \% \text{ yr}^{-1}$ ,  $R = -0.96$ ,  $P < 0.01$ ) in spring during 2012–2017, and  $-0.67 \text{ ppb yr}^{-1}$  ( $-4.5 \% \text{ yr}^{-1}$ ,  $R = -0.87$ ,  
152  $P = 0.01$ ) in summer during 2011–2016.

## 153 **4 Discussion**

### 154 **4.1 The influence of emission control on long-term trends of NO<sub>x</sub> and SO<sub>2</sub>**

155 The annual mean and the 95th percentile of SO<sub>2</sub> mixing ratios at SDZ from 2004 to 2016 were significantly  
156 correlated with the annual SO<sub>2</sub> emissions in North China with correlation coefficients of 0.85 ( $P < 0.01$ ) and 0.88 ( $P$   
157  $< 0.01$ ), respectively. The decreasing rates of annual mean and 95th percentile of SO<sub>2</sub> mixing ratios from 2004 to



158 2016 at SDZ were  $-6.1\% \text{ yr}^{-1}$  and  $-6.2\% \text{ yr}^{-1}$ , respectively, which were higher than the trend ( $-3.1\% \text{ yr}^{-1}$ ) of the  
159 annual  $\text{SO}_2$  emission in the NCP, but very close to the trend ( $-6.3\% \text{ yr}^{-1}$ ) of the annual  $\text{SO}_2$  emission in Beijing.  
160 This indicated that surface  $\text{SO}_2$  mixing ratios at SDZ were more influenced by the emission in Beijing than other  
161 provinces in the NCP.

162 There was a lag between the variation of  $\text{SO}_2$  mixing ratios and the emissions (Fig. 5a,b; Fig. S1a,b), which  
163 indicated the complexity of the effect of reducing  $\text{SO}_2$  emission on  $\text{SO}_2$  mixing ratios. The effectiveness and timing  
164 of pollution control policies, as well as the change of meteorology year by year, would cause their asynchronous  
165 trends.

166 Taking 2008 as the base year, a stronger decreasing trend of  $-7.4\% \text{ yr}^{-1}$  ( $R = -0.95$ ,  $P < 0.01$ ) from 2008 to 2016 for  
167 the annual mean  $\text{SO}_2$  mixing ratio can be found, as well as a significant decreasing rate of ( $-4.5\% \text{ yr}^{-1}$ ,  $R = -0.81$ ,  $P$   
168  $< 0.01$ ) for the annual 5 % percentile of  $\text{SO}_2$  mixing ratios. More strict emission control measures had been  
169 implemented for the 2008 Beijing Olympic Games, where the  $\text{SO}_2$  pollution control had long-term effects and  
170 benefits as Lin et al. (2012) had pointed out. An assessment by the United Nations Environment Programme  
171 reported that the significant decline in  $\text{SO}_2$  mixing ratios and emissions from 1997–2017 was largely due to the  $\text{SO}_2$   
172 control measures in Beijing and the surrounding areas, especially the transformation of coal-fired boilers, energy  
173 structure adjustments and the end treatment of  $\text{SO}_2$  tail gas (UN Environment, 2019). The  $\text{SO}_2$  observation at SDZ  
174 background site confirmed the effect of  $\text{SO}_2$  reduction.

175 After 2010, the annual mean and 95th percentile of  $\text{NO}_x$  mixing ratios correlated significantly ( $R = 0.94$ ,  $P < 0.01$   
176 and  $R = 0.82$ ,  $P < 0.05$ , respectively) with the annual  $\text{NO}_x$  emission in North China, but the  $\text{NO}_x$  mixing ratios  
177 exhibited more fluctuations than  $\text{NO}_x$  emissions (Fig. 5c, 5d). As shown in Fig. S1c and S1d, the annual mean  $\text{NO}_x$   
178 mixing ratios were also significantly correlated with the  $\text{NO}_x$  emission in Beijing ( $R = 0.93$ ,  $P < 0.01$ ) from 2010 to  
179 2016 (Fig. S1c). However, the 95th percentile of  $\text{NO}_x$  did not show a significant correlation ( $R = 0.80$ ,  $P = 0.06$ ) (Fig.  
180 S1d), indicating that high values of  $\text{NO}_x$  at SDZ may be much more affected by  $\text{NO}_x$  emissions from other North  
181 China regions than Beijing. The decreasing rates of  $-4.8\% \text{ yr}^{-1}$  ( $R = -0.92$ ,  $P < 0.01$ ) for the annual mean and  
182  $-4.5\% \text{ yr}^{-1}$  ( $R = -0.82$ ,  $P < 0.05$ ) for the 95th percentile  $\text{NO}_x$  mixing ratios from 2011 to 2016 at SDZ were lower  
183 than the one ( $-8.8\% \text{ yr}^{-1}$ ,  $R = -0.94$ ,  $P < 0.01$ ) for the annual  $\text{NO}_x$  emission in the NCP and ( $-9.0\% \text{ yr}^{-1}$ ,  $R = -0.96$ ,  
184  $P < 0.01$ ) in Beijing. Unlike the annual mean or 95th percentile value, the 5th percentile of  $\text{NO}_x$  mixing ratios from  
185 2011 to 2016 did not exhibit a significant trend ( $-5.0\% \text{ yr}^{-1}$ ,  $R = -0.54$ ,  $P = 0.27$ ) at SDZ.

186 It indicated that surface  $\text{NO}_x$  mixing ratios at SDZ was relatively weakly influenced by the emission reduction in  
187 Beijing and its surrounding areas in the NCP compared with the condition of  $\text{SO}_2$ , probably because there were



188 more emission sources for NO<sub>x</sub> than for SO<sub>2</sub>. For example, although the coal-burning source pollution control  
189 measures adopted in the *the Clean Air Action* have helped to reduce NO<sub>x</sub> emissions, the increase in the amount of  
190 motor vehicles led to an increase in NO<sub>x</sub> emission from the traffic (Fontes et al., 2018; Sun et al., 2018; Zhang et al.,  
191 2019; Zhang et al., 2020). In addition, the change of atmospheric transport conditions and the expansion of urban  
192 scale may lead to the downward trend of NO<sub>x</sub>, but not as obvious as that of SO<sub>2</sub> at SDZ (Lin et al., 2012).  
193 Fortunately, NO<sub>x</sub> pollution control measures on coal-burning source and vehicle pollution had also begun to achieve  
194 more significant outcome since 2011 (Krotkov et al., 2016; UN Environment, 2019). Especially, vehicle pollution  
195 control was strengthened through the improvement of oil quality and promotion of new energy vehicles. As a result,  
196 Beijing's motor vehicle growth rate decreased from 19.7 % in 2010 to 3.6 % in 2011 and the number of new energy  
197 vehicles had an increase of 431 % from 2013 to 2016 (Figure S2).

#### 198 4.2 Variations in NO<sub>x</sub> and SO<sub>2</sub> mixing ratios in different periods

199 We regrouped the NO<sub>x</sub> and SO<sub>2</sub> data into 4 subsets in 4 different time stages (Stage I: 2005–2008, Stage II:  
200 2009–2012, Stage III: 2013–2014, and Stage IV: 2015–2017). Key pollution control measures had been  
201 implemented in different stages, e.g., emission controls for the 2008 Beijing Olympic Games, *the State Council Air*  
202 *Pollution Prevention and Control Action Plan (Action Plan 2013–2017)* and *Beijing 2013–2017 Clean Air Action*  
203 *Plan*. Since 2015, the government of Beijing–Tianjin–Hebei region has promoted the application of electric energy  
204 substitution using electric energy instead of traditional fossil energy (Wang et al., 2020).

205 The average diurnal variations in SO<sub>2</sub> and NO<sub>x</sub> at SDZ in four stages were shown in Fig. 7 and Fig. S3. The SO<sub>2</sub>  
206 levels and their amplitudes of the average diurnal variation continued to decrease as the stage time went by. The  
207 diurnal amplitude of SO<sub>2</sub> was 4.16 ppb in Stage I and 0.94 ppb in Stage IV. The peak time of SO<sub>2</sub> in Stage IV  
208 appeared at 11:00 instead of the former 16:00. The peak value decreased significantly, from 9.38 ppb in Stage I to  
209 3.19 ppb in Stage IV, with a factor of –66.0 %. This phenomenon indicated that the control measures implemented  
210 in the period 2013–2017 have not only had notable effects in reducing emissions from power plants, but also had  
211 significant achievement in the emission control of non-electric industries such as industrial boilers and kilns (Zhang  
212 et al., 2019), which made the emission intensity of SO<sub>2</sub> pollutants from elevated sources weaker than that in the  
213 Stage I.

214 Different from SO<sub>2</sub>, the average diurnal of NO<sub>x</sub> mixing ratios did not show a gradual decrease over time and with  
215 values of Stage II > Stage III > Stage I > Stage IV. In addition, the diurnal variations and the diurnal amplitude of  
216 NO<sub>x</sub> did not change much with the daily amplitudes being about 8.52 ppb. The peak and valley appeared





217 respectively at about 2:00 and at about 13:00 in 4 stages. The reason for the increase of  $\text{NO}_x$  in Stage II may be due  
218 to the fact that the pollution control measures implemented in Beijing and other places have much more effective on  
219  $\text{SO}_2$  rather than  $\text{NO}_x$ . At the same time, the amount of motor vehicles has been rapidly increasing, resulting in an  
220 increase in  $\text{NO}_x$  emissions from vehicle exhaust.

221 Figure 8 is the rose maps of  $\text{SO}_2$  and  $\text{NO}_x$  mixing ratios in 4 different time periods (Figure S4 and S5 are rose maps  
222 in different seasons, Table S1 is frequency distributions of wind directions in different stages). High  $\text{NO}_x$  values  
223 were in broader wind sectors except NW–NNW–N–NNE, whereas high  $\text{SO}_2$  values were mainly in  
224 W–WSW–SW–SSW sectors.

225 Except for the SSW sector,  $\text{SO}_2$  mixing ratios in other wind directions showed a decreasing trend over stages. Both  
226 the severely polluted areas and the slightly polluted areas have the same characteristics of decreasing in  $\text{SO}_2$  level  
227 over time (Table 3). Unlike the highest  $\text{SO}_2$  mixing ratio being in Stage I (2005–2008), the highest  $\text{NO}_x$  mixing  
228 ratios was in Stage II (2009–2012). The overall levels of  $\text{SO}_2$  and  $\text{NO}_x$  in the Stage IV reached the lowest value  
229 among the four stages. Compared with those at the stage with the highest mixing ratios of  $\text{NO}_x$  and  $\text{SO}_2$ , the  
230 reduction ranges in Stage IV are 52.2 %–76.4 % for  $\text{SO}_2$  and 3.8 %–45.3 % for  $\text{NO}_x$  in different wind sectors. Much  
231 more reduction in  $\text{SO}_2$  than  $\text{NO}_x$  indicates that the electric energy substitution policy in Beijing–Tianjin–Hebei  
232 region has much more effective on  $\text{SO}_2$  reduction than  $\text{NO}_x$ .

233 The  $\text{SO}_2/\text{NO}_x$  ratio, obtained from the reduced major axis regression of the daily mean  $\text{SO}_2$  and  $\text{NO}_x$  mixing ratios,  
234 exhibited a significant change from 0.84 during 2005–2008 to 0.30 during 2015–2017. The possible reason for this  
235 phenomenon was that the control measures including the upgrading of end treatment facilities of coal-fired power  
236 plants, the conversion of coal to clean energy, and the elimination of coal-fired boilers, which were taken in the early  
237 stage of *the Clean Air Action*, had greatly reduced  $\text{SO}_2$  emissions rather than  $\text{NO}_x$ . Another reason should be an  
238 increase in the number of motor vehicles (Figure S2) and relatively more difficult in emission control on the mobile  
239 sources.

240 In the period of 2005–2012, the construction of new power plants and the amount of motor vehicle ownership  
241 rapidly increased in the city. During this period, flue gas desulfurization devices have been widely used (Zhao et al.,  
242 2008). However, the main management measures that required power plants to deploy denitrification devices for  
243 reducing  $\text{NO}_x$  emissions, were not be implemented until 2012, resulting in the increase of nitrogen oxide emissions  
244 (Wang et al., 2010; Wang and Hao, 2012; Liu et al., 2016), and the contribution to the transport of  $\text{NO}_x$  to SDZ  
245 during this period.



246 **4.3 The different diurnal behaviors in SO<sub>2</sub> and NO<sub>x</sub> mixing ratios and their source origin**

247 The seasonal variations in SO<sub>2</sub> and NO<sub>x</sub> mixing ratios exhibited a similar pattern with high in winter and low in  
248 summer, and their daily mean values had a significant correlation ( $R = 0.59$ ,  $P < 0.01$ ). However, the diurnal  
249 variations in SO<sub>2</sub> and NO<sub>x</sub> mixing ratios were greatly different in all seasons (Figure 9). The SO<sub>2</sub> mixing ratios were  
250 higher during the daytime and lower during the nighttime, while the NO<sub>x</sub> mixing ratios showed an opposite pattern.

251 The different diurnal behaviors in SO<sub>2</sub> and NO<sub>x</sub> at SDZ might indicate a different origin of SO<sub>2</sub> and NO<sub>x</sub>.

252 Due to the diurnal variation in the boundary layer, the mixing depth is higher during the daytime and the convective  
253 mixing is strong, which is conducive to the dilution and diffusion of pollutants. The photochemical reaction during  
254 the daytime is also conducive to the chemical transformation of pollutants. At night, the pollutants are easy to  
255 accumulate because of lower mixing depth and no photochemical processes. Therefore, the concentration of primary  
256 pollutants exhibits higher values during the nighttime and lower during the daytime in general. But the situation for  
257 SO<sub>2</sub> at SDZ was different. The higher SO<sub>2</sub> mixing ratios during the daytime suggested two possible mechanisms: (1)  
258 an elevated level of SO<sub>2</sub> aloft, which could be mixed downward to the ground due to the evolution of atmospheric  
259 boundary layer, causing higher ground-level SO<sub>2</sub> concentrations in the daytime. (2) upwind SO<sub>2</sub> sources and  
260 transport of plumes in the daytime.

261 As SDZ is located on the north side of a valley with a northeast-southwest orientation, its dominant wind directions  
262 were from southwest and northeast with regular changes in diurnal wind directions (Figure S6). The southwest  
263 mouth of the valley is open to the NCP, so it is easily influenced by the air masses from the south polluted areas,  
264 like urban Beijing. As a result, the concentration rose maps of pollutants exhibited higher values in the southwest  
265 sectors than other sectors (Lin et al., 2008; Meng et al., 2009). If only due to the influence by advection transport,  
266 the diurnal variations in SO<sub>2</sub> and NO<sub>x</sub> at SDZ should be similar. However, the two show obvious differences. The  
267 higher SO<sub>2</sub> mixing ratios during the daytime indicates an elevated level of SO<sub>2</sub> in a high air layer, which can be  
268 exchanged to the surface under the evolution of atmospheric boundary layer, causing a higher SO<sub>2</sub> value in the  
269 daytime. The 'unusual' phenomenon of the diurnal change in SO<sub>2</sub> has been noticed and explained by studies (Lin et  
270 al., 2008; Chen et al., 2009; Xu et al., 2014), but it lacked direct vertical profile measurements to support this  
271 explanation. The daytime peak of SO<sub>2</sub> was not only found at SDZ, but also at different sites in urban and rural areas  
272 in North China (Lin et al., 2012) and in the background area of the YRD (Qi et al., 2012). This may be related to the  
273 fact that SO<sub>2</sub> is mainly emitted from elevated sources (Lin et al., 2012; Xu et al., 2014).

274 In addition, it can be seen that the NO<sub>x</sub> mixing ratios began to rise around noontime when the mixing depth was still



275 elevating (Figure 9). Obviously,  $\text{NO}_x$  was affected by the transport of pollutants in the southern polluted area during  
276 the noontime when the WD changed into southwest wind (Figure S6). However,  $\text{SO}_2$  maintained a relatively high  
277 value instead of increasing significantly, indicating that  $\text{SO}_2$  mixing ratios was still mainly affected by downward  
278 mixing of  $\text{SO}_2$ -richer air.

### 279 **Conclusion**

280 Measurements of surface  $\text{NO}_x$  and  $\text{SO}_2$  mixing ratios at SDZ regional atmospheric background site in the North  
281 China Plain from the period 2005–2017, together with ancillary data, were summarized and used to study their  
282 long-term trends and influencing factors. The average values  $\pm 1\sigma$  (standard deviation) of  $\text{SO}_2$  and  $\text{NO}_x$  mixing  
283 ratios were  $5.7 \pm 8.4$  ppb and  $14.2 \pm 12.4$  ppb, respectively. The seasonal variation in  $\text{SO}_2$  and  $\text{NO}_x$  at SDZ showed a  
284 similar pattern with high values in winter and low in summer, but the diurnal variations in  $\text{SO}_2$  and  $\text{NO}_x$  mixing ratio  
285 exhibited greatly different for all seasons. The  $\text{SO}_2$  mixing ratios were higher during the daytime and lower during  
286 the nighttime, while the  $\text{NO}_x$  mixing ratios showed higher values during the nighttime and lower during the daytime.  
287 The different diurnal behaviors in  $\text{SO}_2$  and  $\text{NO}_x$  at SDZ indicated a different origin of  $\text{SO}_2$  and  $\text{NO}_x$ .  
288 Overall, the annual mean  $\text{SO}_2$  exhibited a significant decreasing trend of  $-0.36$  ppb  $\text{yr}^{-1}$  ( $-6.1$  %  $\text{yr}^{-1}$ ,  $R = -0.84$ ,  $P <$   
289  $0.01$ ) from 2004 to 2016 and a greater decreasing trend of  $-0.56$  ppb  $\text{yr}^{-1}$  ( $-7.4$  %  $\text{yr}^{-1}$ ,  $R = -0.95$ ,  $P < 0.01$ ) from  
290 2008 to 2016. The decreasing rates of annual mean and 95th percentile of  $\text{SO}_2$  mixing ratios from 2004 to 2016 at  
291 SDZ are very close to the one ( $-6.3$  %  $\text{yr}^{-1}$ ) of the annual  $\text{SO}_2$  emission in Beijing. The annual mean of  $\text{NO}_x$  showed  
292 a fluctuating rise of  $+0.37$  ppb  $\text{yr}^{-1}$  ( $+3.4$  %  $\text{yr}^{-1}$ ,  $R = 0.38$ ,  $P = 0.40$ ) from 2005 to 2010, reaching the peak value  
293 ( $16.93$  ppb) in 2010, and then exhibited an extremely significant fluctuating downward trend of  $-0.77$  ppb  $\text{yr}^{-1}$   
294 ( $-4.5$  %  $\text{yr}^{-1}$ ,  $R = 0.95$ ,  $P < 0.01$ ) from 2010 to 2016. After 2010, the annual mean and 95 % percentile of  $\text{NO}_x$   
295 mixing ratios correlated significantly ( $R = 0.94$ ,  $P < 0.01$  and  $R = 0.82$ ,  $P < 0.05$ , respectively) with the annual  $\text{NO}_x$   
296 emission in North China. The decreasing rates of  $-4.8$  %  $\text{yr}^{-1}$  ( $R = -0.92$ ,  $P < 0.01$ ) for the annual mean and  $-4.5$  %  
297  $\text{yr}^{-1}$  ( $R = -0.82$ ,  $P < 0.05$ ) for the 95th percentile  $\text{NO}_x$  mixing ratios from 2011 to 2016 at SDZ are lower than the  
298 one ( $-8.8$  %  $\text{yr}^{-1}$ ,  $R = -0.94$ ,  $P < 0.01$ ) for the annual  $\text{NO}_x$  emission in the NCP and ( $-9.0$  %  $\text{yr}^{-1}$ ,  $R = -0.96$ ,  $P <$   
299  $0.01$ ) in Beijing. It indicated that surface  $\text{NO}_x$  mixing ratios at SDZ had weaker influence than  $\text{SO}_2$  by the emission  
300 reduction in Beijing and its surrounding areas in NCP. The increase in the amount of motor vehicles and the weak  
301 effectiveness of traffic restrictions have caused motor vehicle emissions on  $\text{NO}_x$ .



302 **Data availability.** The data of stationary measurements are available upon request to the contact author Weili Lin  
303 (linwl@muc.edu.cn).

304 **Author contributions.** XL wrote the paper, WL developed the idea, formulated the research goals, and edited the  
305 paper. LR, XX and ZQ edited the paper. WL, FD, DH, LZ, QS and YW carried out the measurement of NO<sub>x</sub> and  
306 SO<sub>2</sub>, and analysed the meteorological data.

307 **Competing interests.** The authors declare that they have no conflict of interest.

308 **Acknowledgements.** This study was funded by the National Natural Science Foundation of China (Grant No.  
309 91744206) and the Open Fund of Shangdianzi Atmospheric Background Station (SDZ2020615).

## 310 References

311 Cai, K., Zhang, Q., Li, S., Li, Y., and Ge, W.: Spatial-temporal variations in NO<sub>2</sub> and PM<sub>2.5</sub> over the Chengdu–Chongqing  
312 economic zone in China during 2005 – 2015 based on satellite remote sensing, *Sensors-Basel*, 18, 3950,  
313 <https://doi.org/10.3390/s18113950>, 2018.

314 Chen, L.: Measure and study on the atmospheric pollutants in three typical regional background stations of China (in Chinese),  
315 Master, Lanzhou University, 2012.

316 Chen, C.: Analysis of atmospheric pollutants characteristics in the typical suburban station of North China (in Chinese), Master,  
317 Nanjing University of Information Science and Technology, 2017.

318 Chen, T., Chang, K., and Tsai, C.: Modeling approach for emissions reduction of primary PM<sub>2.5</sub> and secondary PM<sub>2.5</sub> precursors  
319 to achieve the air quality target, *Atmos. Res.*, 192, 11-18, <https://doi.org/10.1016/j.atmosres.2017.03.018>, 2017.

320 Chen, Y., Zhao, C., Qiang, Z., Deng, Z., Huang, M., and Ma, X.: Aircraft study of mountain chimney effect of Beijing, China, J.  
321 *Geophys. Res-atmos.*, 114, D8306, <https://doi.org/10.1029/2008JD010610>, 2009.

322 Cheng, M., Pan, Y., Wang, H., Liu, Q., and Wang, Y.: On-line measurement of water-soluble composition of particulate matter  
323 in Beijing, *Environ. Sci.*, 34, 2943-2949, 2013.

324 Cheng, N., Chen, T., Zhang, D., Li, Y., Sun, F., Wei, Q., Liu, J., Liu, B., and Sun, R.: Air quality characteristics in Beijing during  
325 Spring Festival in 2015 (in Chinese), *Environ. Sci.*, 36, 3150-3158, <https://doi.org/10.13227/j.hjkk.2015.09.005>, 2015.



- 326 Cheng, L., Ji, D., He, J., Li, L., Du, L., Cui, Y., Zhang, H., Zhou, L., Li, Z., and Zhou, Y.: Characteristics of air pollutants and  
327 greenhouse gases at a regional background station in Southwestern China, *Aerosol Air Qual. Res.*, 19, 1007-1023,  
328 <https://doi.org/10.4209/aaqr.2018.11.0397>, 2019.
- 329 Fontes, T., Li, P., Barros, N., and Zhao, P.: A proposed methodology for impact assessment of air quality traffic-related measures:  
330 The case of PM<sub>2.5</sub> in Beijing, *Environ. Pollut.*, 239, 818-828, <https://doi.org/10.1016/j.envpol.2018.04.061>, 2018.
- 331 Gao, J., Zhang, Y., Wang, S., Chai, F., and Chen, Y.: Study on the characteristics and formation of a multi-day haze in October  
332 2011 in Beijing (in Chinese), *Res. Environ. Sci.*, 25, 1201-1207, <https://doi.org/CNKI:SUN:HJKX.0.2012-11-002>, 2012.
- 333 Krotkov, N. A., McLinden, C. A., Li, C., Lamsal, L. N., Celarier, E. A., Marchenko, S. V., Swartz, W. H., Bucsela, E. J., Joiner, J.,  
334 and Duncan, B. N.: Aura OMI observations of regional SO<sub>2</sub> and NO<sub>2</sub> pollution changes from 2005 to 2015, *Atmos. Chem.*  
335 *Phys.*, 16, 4605-4629, <https://doi.org/10.5194/acp-16-4605-2016>, 2016.
- 336 Li, F., Tan, H., Deng, X., Deng, T., Xu, W., Ran, L., and Zhao, C.: Characteristics analysis of sulfur dioxide in Pearl River Delta  
337 from 2006 to 2010 (in Chinese), *Environ. Sci.*, 5, 1530-1537, <https://doi.org/CNKI:SUN:HJKZ.0.2015-05-003>, 2015.
- 338 Li, Y., Wang, J., Han, T., Wang, Y., He, D., Quan, W., and Ma, Z.: Using multiple linear regression method to evaluate the  
339 impact of meteorological conditions and control measures on air quality in Beijing during APEC 2014 (in Chinese), *Environ.*  
340 *Sci.*, 40, 1024-1034, <https://doi.org/10.13227/j.hjx.201807044>, 2019.
- 341 Li, W., Shao, L., Wang, W., Li, H., Wang, X., Li, Y., Li, W., Jones, T., and Zhang, D.: Air quality improvement in response to  
342 intensified control strategies in Beijing during 2013 – 2019, *Sci. Total. Environ.*, 744, 140776,  
343 <https://doi.org/10.1016/j.scitotenv.2020.140776>, 2020.
- 344 Lin, W., Xu, X., Zhang, X., and Tang, J.: Contributions of pollutants from North China Plain to surface ozone at the Shangdianzi  
345 GAW station, *Atmos. Chem. Phys.*, 8, 5889-5898, <https://doi.org/10.5194/acp-8-5889-2008>, 2008.
- 346 Lin, W., Xu, X., Ge, B., and Zhang, X.: Characteristics of gaseous pollutants at Gucheng, a rural site southwest of Beijing, *J.*  
347 *Geophys. Res-atmos.*, 114, D14G, <https://doi.org/10.1029/2008JD010339>, 2009.
- 348 Lin, W., Xu, X., Yu, D., Dai, X., Zhang, Z., Meng, Z., and Wang, Y.: Quality control for reactive gases observation at  
349 Longfengshan regional atmospheric background monitoring station (in Chinese), *Meteorol. Mon.*, 35, 93-100,  
350 <https://doi.org/10.7519/j.issn.1000-0526.2009.11.012>, 2009.
- 351 Lin, W., Xu, X., Ge, B., and Liu, X.: Gaseous pollutants in Beijing urban area during the heating period 2007–2008: variability,  
352 sources, meteorological, and chemical impacts, *Atmos. Chem. Phys.*, 11, 6919-6959,  
353 <https://doi.org/10.5194/acp-11-8157-2011>, 2011.



- 354 Lin, W., Xu, X., Sun, J., Li, Y., and Meng, Z.: Background concentrations of reactive gases and the impacts of long-range  
355 transport at the Jinsha regional atmospheric background station, *Sci. China Earth Sci.*, 54, 1604-1613,  
356 <https://doi.org/10.1007/s11430-011-4205-2>, 2011.
- 357 Lin, W., Xu, X., Ma, Z., Zhao, H., Liu, X., and Wang, Y.: Characteristics and recent trends of sulfur dioxide at urban, rural, and  
358 background sites in North China: Effectiveness of control measures, *J. Environ. Sci.*, 24, 34-49,  
359 [https://doi.org/10.1016/s1001-0742\(11\)60727-4](https://doi.org/10.1016/s1001-0742(11)60727-4), 2012.
- 360 Lin, W., Ma, Z., Pu, W., Gao, W., Ma, Q., and Yu, D.: Air Composition-Quality control for observation data-Reactive gases.  
361 Meteorological industry Standard of the People's Republic of China (QX/T 510–2019), 2019.
- 362 Liu, J., Zhang, X., Xu, X., and Xu, H.: Comparison analysis of variation characteristics of SO<sub>2</sub>, NO<sub>x</sub>, O<sub>3</sub> and PM<sub>2.5</sub> between rural  
363 and urban areas, Beijing (in Chinese), *Environ. Sci.*, 29, 1059-1065, <https://doi.org/10.3321/j.issn:0250-3301.2008.04.036>,  
364 2008.
- 365 Liu, R., Han, Z., and Li, J.: Analysis of meteorological characteristics during winter haze events in Beijing (in Chinese), *Clim.*  
366 *Environ. Res.*, 19, 164-172, <https://doi.org/10.3878/j.issn.1006-9585.2014.13224>, 2014.
- 367 Liu, X., Xu, X., Zhao, H., and Lin, W.: Characteristics of NO<sub>x</sub> and CO emission on the three sites in Beijing and its surrounding  
368 areas (in Chinese), *J. Saf. Environ.*, 14, 252-257, <https://doi.org/10.13637/j.issn.1009-6094.2014.06.056>, 2014.
- 369 Liu, F., Zhang, Q., Van, D. A. R. J., Zheng, B., Tong, D., Yan, L., Zheng, Y., and He, K.: Recent reduction in NO<sub>x</sub> emissions  
370 over China: synthesis of satellite observations and emission inventories, *Environ. Res. Lett.*, 11, 3945-3950,  
371 <https://doi.org/10.1088/1748-9326/11/11/114002>, 2016.
- 372 Luo, X., Pan, Y., Goulding, K., Zhang, L., Liu, X., and Zhang, F.: Spatial and seasonal variations of atmospheric sulfur  
373 concentrations and dry deposition at 16 rural and suburban sites in China, *Atmos. Environ.*, 146, 79-89,  
374 <https://doi.org/10.1016/j.atmosenv.2016.07.038>, 2016.
- 375 Meng, X., Wang, P., Wang, G., Yu, H., and Zong, X.: Variation and transportation characteristics of SO<sub>2</sub> in winter over Beijing  
376 and its surrounding areas (in Chinese), *Clim. Environ. Res.*, 14, 83-91, <https://doi.org/10.3878/j.issn.1006-9585.2009.03.08>,  
377 2009.
- 378 Meng, Z., Xu, X., Yan, P., Ding, G., Tang, J., Lin, W., Xu, X., and Wang, S.: Characteristics of trace gaseous pollutants at a  
379 regional background station in Northern China, *Atmos. Chem. Phys.*, 9, 927-936, <https://doi.org/10.5194/acp-9-927-2009>,  
380 2009.
- 381 Qi, H., Lin, W., Xu, X., and Yu, X.: Significant downward trend of SO<sub>2</sub> observed from 2005 to 2010 at a background station in  
382 the Yangtze Delta region, China, *Sci. China. Chem.*, 55, 1451-7291, <https://doi.org/10.1007/s11426-012-4524-y>, 2012.



- 383 Qiu, X., Duan, L., Cai, S., Yu, Q., Wang, S., Chai, F., Gao, J., Li, Y., and Xu, Z.: Effect of current emission abatement strategies  
384 on air quality improvement in China: A case study of Baotou, a typical industrial city in Inner Mongolia, *J. Environ.*  
385 *Sci.-China.*, 57, 383-390, <https://doi.org/10.1016/j.jes.2016.12.014>, 2017.
- 386 Shao, M., Tang, X., Zhang, Y., and Li, W.: City clusters in China: air and surface water pollution, *Front. Ecol. Environ.*, 4,  
387 353-361, [https://doi.org/10.1890/1540-9295\(2006\)004\[0353:CCICAA\]2.0.CO;2](https://doi.org/10.1890/1540-9295(2006)004[0353:CCICAA]2.0.CO;2), 2006.
- 388 Su, B., Liu, X., and Tao, J.: Pollution characteristics of SO<sub>2</sub>, NO<sub>x</sub> and CO in forest and mountain background region of East  
389 China (in Chinese), *Environ. Monit. China.*, 29, 15-21, <https://doi.org/10.3969/j.issn.1002-6002.2013.06.004>, 2013.
- 390 Song, C., Li, R., Jianjun, H., Wu, L., and Mao, H.: Analysis of pollution characteristics of NO, NO<sub>2</sub> and O<sub>3</sub> at urban area of  
391 Langfang, Hebei (in Chinese), *J. Environ. Sci.-China.*, 36, 2903-2912, <https://doi.org/CNKI:SUN:ZGHJ.0.2016-10-004>, 2016.
- 392 Sun, C., Luo, Y., and Li, J.: Urban traffic infrastructure investment and air pollution: Evidence from the 83 cities in China, *J.*  
393 *Clean. Prod.*, 172, 488-496, <https://doi.org/10.1016/j.jclepro.2017.10.194>, 2018.
- 394 Shikwambana, L., Mhangara, P., and Mbatha, N.: Trend analysis and first time observations of sulphur dioxide and nitrogen  
395 dioxide in South Africa using TROPOMI/Sentinel-5 P data, *Int. J. Appl. Earth Obs. Geoinf.*, 91, 102130,  
396 <https://doi.org/10.1016/j.jag.2020.102130>, 2020.
- 397 Tang, Y., Zhang, X., Xu, J., Zhao, X., Ma, Z., and Meng, W.: Multi-temporal scale variations of atmospheric pollutants  
398 concentrations in rural and urban areas of Beijing (in Chinese), *Acta Sci. Circumst.*, 36, 2783-2793,  
399 <https://doi.org/10.13671/j.hjkxxb.2016.0003>, 2016.
- 400 UN Environment. A Review of 20 Years' Air Pollution Control in Beijing. United Nations Environment Programme, Nairobi,  
401 Kenya, 2019.
- 402 Wang, S., Streets, D. G., Zhang, Q., He, K., Chen, D., Kang, S., Lu, Z., and Wang, Y.: Satellite detection and model verification  
403 of NO<sub>x</sub> emissions from power plants in Northern China, *Environ. Res. Lett.*, 5, 44007,  
404 <https://doi.org/10.1088/1748-9326/5/4/044007>, 2010.
- 405 Wang, S., and Hao, J.: Air quality management in China: Issues, challenges, and options, *J. Environ. Sci.*, 24, 2-13,  
406 [https://doi.org/10.1016/S1001-0742\(11\)60724-9](https://doi.org/10.1016/S1001-0742(11)60724-9), 2012.
- 407 Wang, Y., Wang, S., Song, F., Yang, J., Zhu, J., and Zhang, F.: Study on the forecast model of electricity substitution potential in  
408 Beijing – Tianjin – Hebei region considering the impact of electricity substitution policies, *Energ. Policy.*, 144, 111686,  
409 <https://doi.org/10.1016/j.enpol.2020.111686>, 2020.
- 410 WMO. 2001. Global Atmosphere Watch Measurements Guide (WMO TD No. 1073). GAW Report No. #171. Geneva,  
411 Switzerland: World Meteorological Organization. Accessed on April 2, 2015. Available at  
412 <ftp://ftp.wmo.int/Documents/PublicWeb/arep/gaw/gaw143.pdf>.

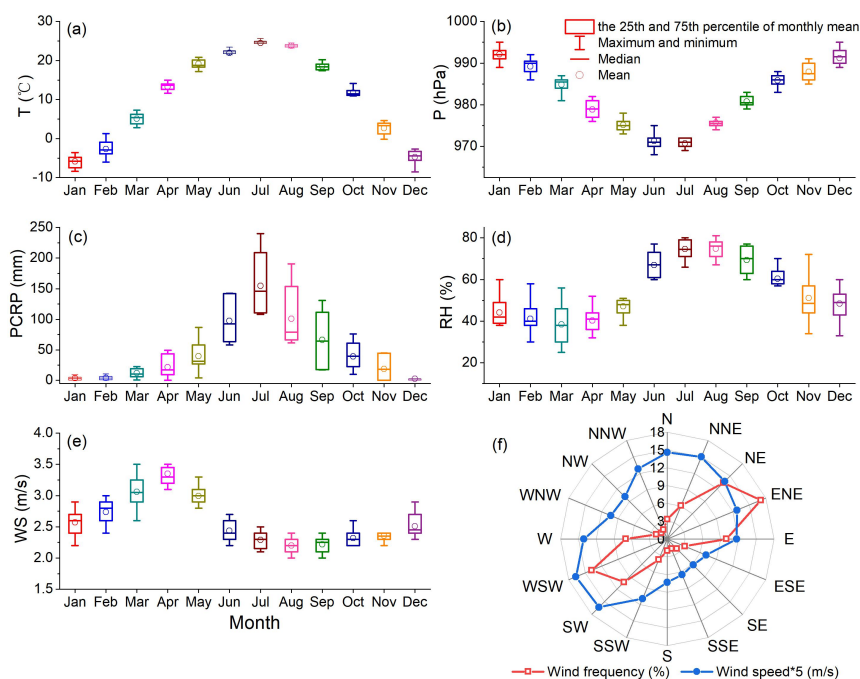


- 413 Wu, D., Xin, J., Sun, Y., Wang, Y., and Wang, P.: Change and analysis of background concentration of air pollutants in North  
414 China during 2008 Olympic Games (in Chinese), *Environ. Sci.*, 31, 1130-1138,  
415 <https://doi.org/CNKI:SUN:HJKZ.0.2010-05-003>, 2010.
- 416 Xu, X., Lin, W., Yan, P., Zhang, Z., and Yu, X.: Long-term changes of acidic gases in China's Yangtze Delta and Northeast  
417 Plain regions during 1994 – 2006 (in Chinese), *Adv. Clim. Chang. Res.*, 4, 195-201,  
418 <https://doi.org/10.3969/j.issn.1673-1719.2008.04.001>, 2008.
- 419 Xu, X., Liu, X., and Lin, W.: Impacts of air parcel transport on the concentrations of trace gases at regional background stations  
420 (in Chinese), *J. Appl. Meteorol. Sci.*, 20, 656-664, <https://doi.org/10.11898/1001-7313.20090602>, 2009.
- 421 Xu, W., Zhao, C., Ran, L., Lin, W., Yan, P., and Xu, X.: SO<sub>2</sub> noontime-peak phenomenon in the North China Plain, *Atmos.*  
422 *Chem. Phys.*, 14, 7757-7768, <https://doi.org/10.5194/acp-14-7757-2014>, 2014.
- 423 Yang, S., Zhao, X., and Liu, N.: Impacting factors of a heavy air pollution process in autumn over Beijing (in Chinese), *J.*  
424 *Meteorol. Environ.*, 13-16, <https://doi.org/10.3969/j.issn.1673-503X.2010.05.003>, 2010.
- 425 Yang, F., Tan, J., Zhao, Q., Du, Z., He, H., Ma, Y., Duan, F., Chen, G., and Zhao, Q.: Characteristics of PM<sub>2.5</sub> speciation in  
426 representative megacities and across China, *Atmos. Chem. Phys.*, 11, 1025-1051, <https://doi.org/10.5194/acp-11-5207-2011>,  
427 2011.
- 428 Yin, Q., Ma, Q., Lin, W., Xu, X., and Yao, J.: Measurement report: Long-term variations in surface NO<sub>x</sub> and SO<sub>2</sub> from 2006 to  
429 2016 at a background site in the Yangtze River Delta region, China, *Atmos. Chem. Phys. Discuss.* [preprint],  
430 <https://doi.org/10.5194/acp-2021-227>, in review, 2021.
- 431 Zhang, X., Zhang, P., Zhang, Y., Li, X., and Qiu, H.: The trend, seasonal cycle, and sources of tropospheric NO<sub>2</sub> over China  
432 during 1997–2006 based on satellite measurement, *Sci China Earth Sci.*, 50, 8, <https://doi.org/10.1007/s11430-007-0141-6>,  
433 2007.
- 434 Zhang, Q., Zheng, Y., Tong, D., Shao, M., Wang, S., Zhang, Y., Xu, X., Wang, J., He, H., Liu, W., Ding, Y., Lei, Y., Li, J.,  
435 Wang, Z., Zhang, X., Wang, Y., Cheng, J., Liu, Y., Shi, Q., Yan, L., Geng, G., Hong, C., Li, M., Liu, F., Zheng, B., Cao, J.,  
436 Ding, A., Gao, J., Fu, Q., Huo, J., Liu, B., Liu, Z., Yang, F., He, K., and Hao, J.: Drivers of improved PM<sub>2.5</sub> air quality in  
437 China from 2013 to 2017, *P. Natl. Acad. Sci. USA.*, 116, 24463-24469, <https://doi.org/10.1073/pnas.1907956116>, 2019.
- 438 Zhang, M., Shan, C., Wang, W., Pang, J., and Guo, S.: Do driving restrictions improve air quality: Take Beijing–Tianjin for  
439 example? *Sci. Total Environ.*, 712, 136408, <https://doi.org/10.1016/j.scitotenv.2019.136408>, 2020.
- 440 Zhao, Y., Wang, S., Duan, L., Lei, Y., Cao, P., and Hao, J.: Primary air pollutant emissions of coal-fired power plants in China:  
441 Current status and future prediction, *Atmos. Environ.*, 42, 8442-8452, <https://doi.org/10.1016/j.atmosenv.2008.08.021>, 2008.



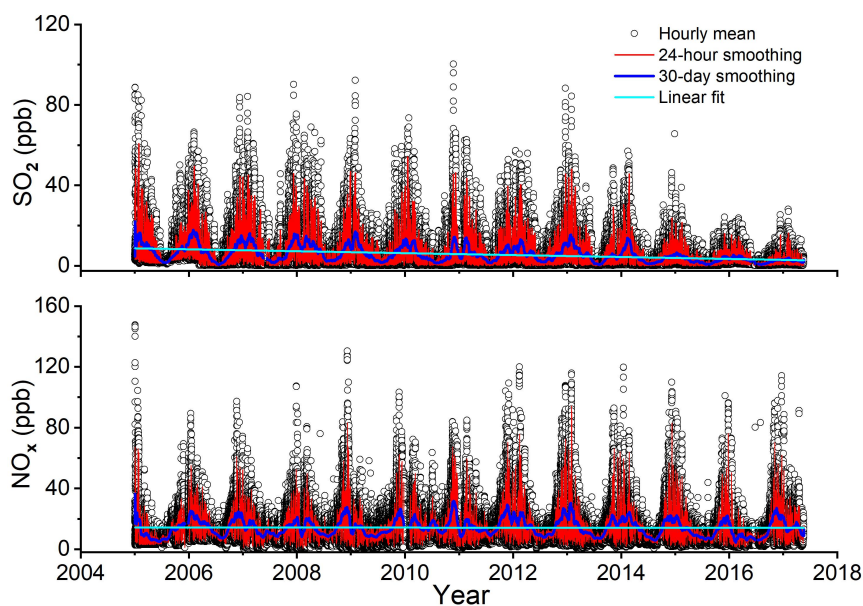


- 442 Zhao, P. S., Dong, F., D, H., Zhao, X. J., Zhang, X. L., Zhang, W. Z., Yao, Q., and Liu, H. Y.: Characteristics of concentrations  
443 and chemical compositions for PM<sub>2.5</sub> in the region of Beijing, Tianjin, and Hebei, China, *Atmos. Chem. Phys.*, 9, 4631-4644,  
444 <https://doi.org/10.5194/acp-13-4631-2013>, 2013.
- 445 Zhao, S., Hu, B., Gao, W., Li, L., Huang, W., Wang, L., Yang, Y., Liu, J., Li, J., Ji, D., Zhang, R., Zhang, Y., and Wang, Y.:  
446 Effect of the "coal to gas" project on atmospheric NO<sub>x</sub> during the heating period at a suburban site between Beijing and  
447 Tianjin, *Atmos. Res.*, 241, 104977, <https://doi.org/10.1016/j.atmosres.2020.104977>, 2020.
- 448 Zhong, Y., Zhou, Y., Cheng, S., Wang, X., and Shao, X.: Comparison analysis of the effect of emission reduction measures for  
449 major events and heavy air pollution in the capital (in Chinese), *Environ. Sci.*, 41, 3449-3457,  
450 <https://doi.org/10.13227/j.hjlx.201910166>, 2020.



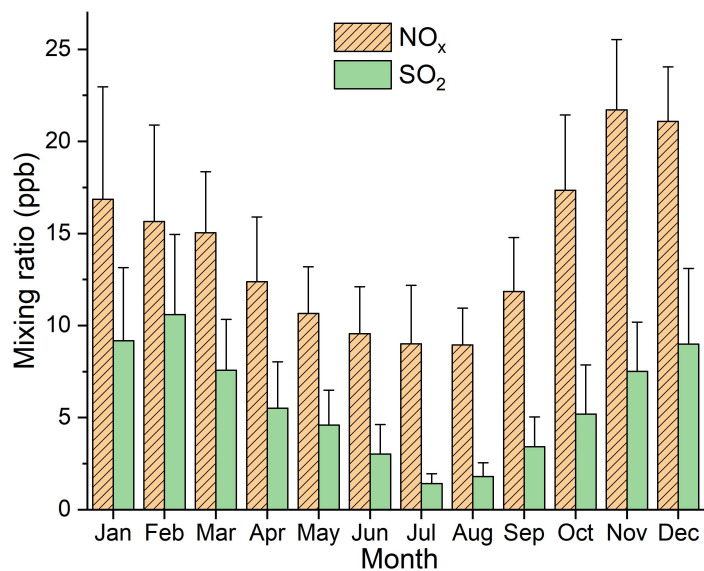
451

**Figure 1.** Monthly variations in (a) air temperature. (b) atmospheric pressure. (c) precipitation. (d) relative humidity. (e) wind speed. (f) wind rose map. at SDZ.



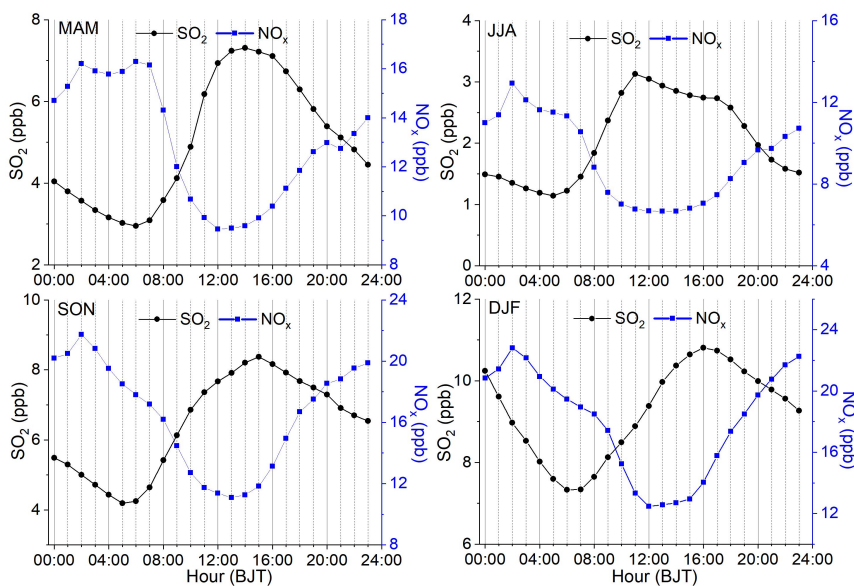
452

**Figure 2.** The time series variations in SO<sub>2</sub> and NO<sub>x</sub> mixing ratios at SDZ.



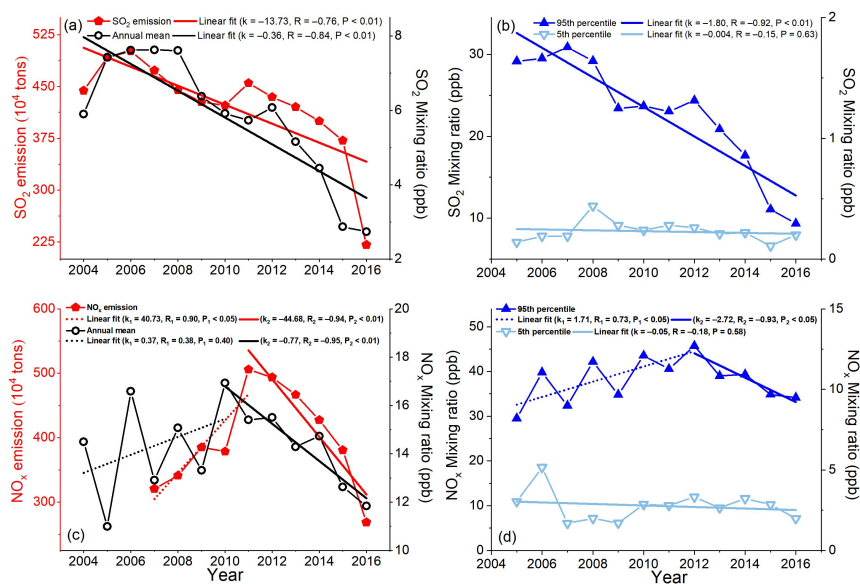
453

**Figure 3.** The average monthly mean of SO<sub>2</sub> and NO<sub>x</sub> mixing ratios with 1  $\sigma$  at SDZ.



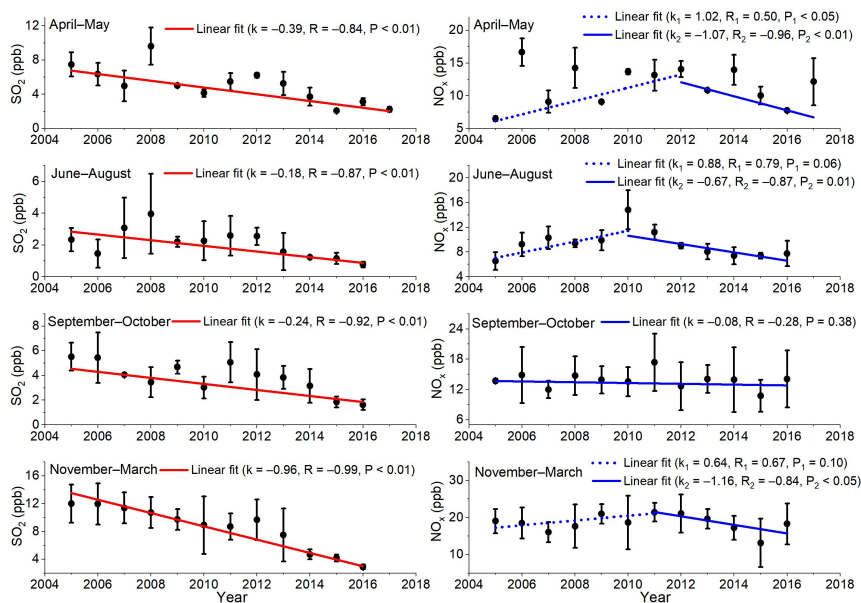
454

**Figure 4.** The Average diurnal variations in SO<sub>2</sub> and NO<sub>x</sub> mixing ratios in four seasons at SDZ.



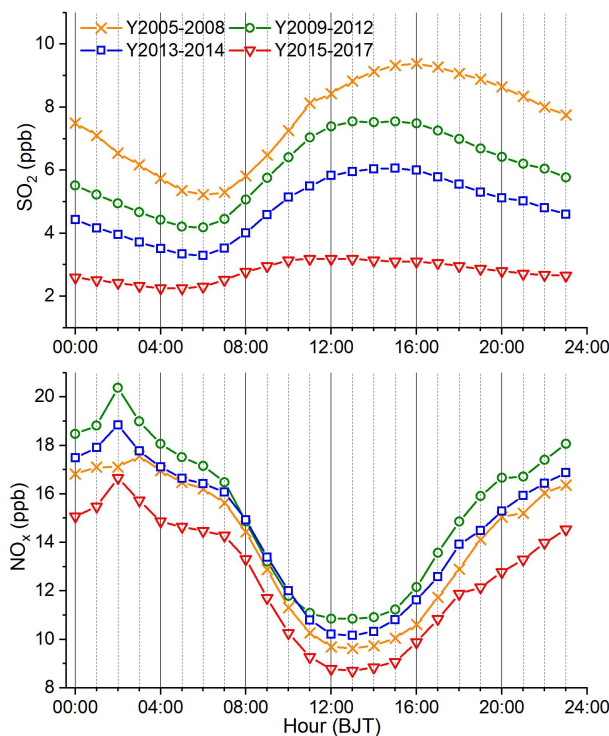
455

**Figure 5.** Annually variations in (a) SO<sub>2</sub> mixing ratios at SDZ and total SO<sub>2</sub> emissions in North China; (b) the 5th and 95th percentile of the hourly mean of SO<sub>2</sub> and SO<sub>2</sub> emissions in North China; (c) NO<sub>x</sub> mixing ratios at SDZ and total NO<sub>x</sub> emissions in North China; (d) the 5th and 95th percentile of the hourly mean of NO<sub>x</sub> and NO<sub>x</sub> emissions in North China. The emission data are from the 2005–2017 Yearbook of National Bureau of Statistics of China and China Statistical Yearbook on Environment provided by Ministry of Ecology and Environment of the People's Republic of China.



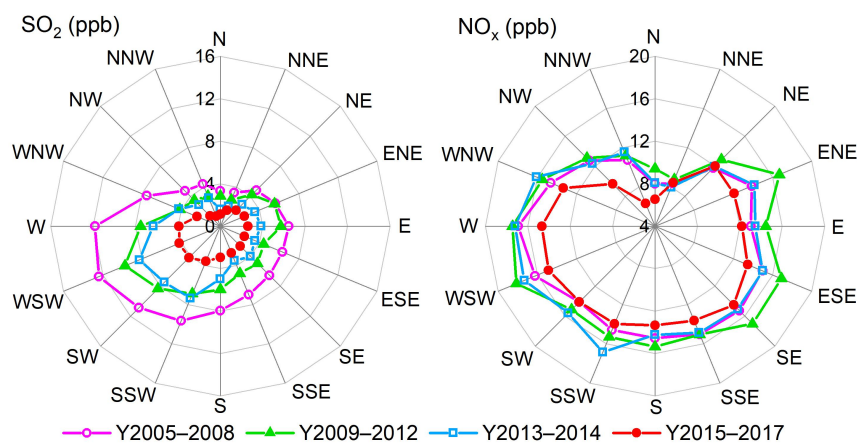
456

**Figure 6.** Long-term variations in monthly mean  $\text{SO}_2$  and  $\text{NO}_x$  mixing ratios with  $\pm 1\sigma$  in different periods at SDZ. Heating period (November–March), spring (April–May), summer (June–August), and autumn (September–October).



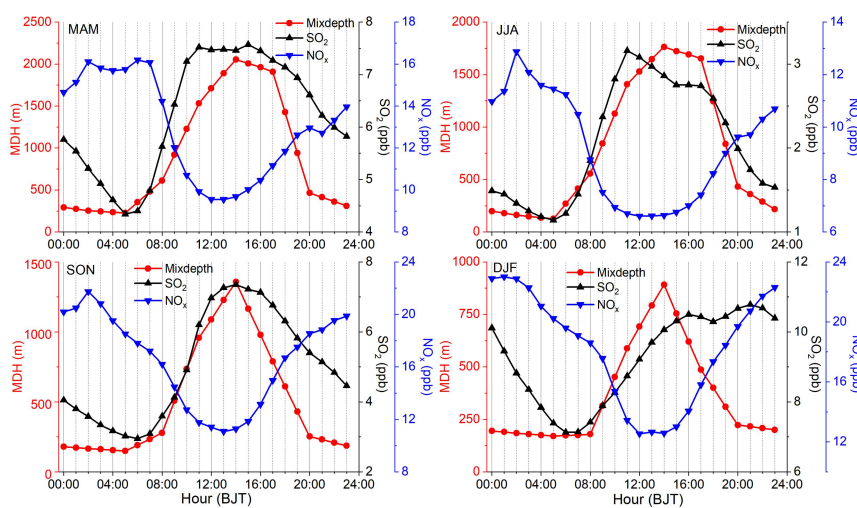
457

**Figure 7.** The average diurnal variations in  $\text{SO}_2$  and  $\text{NO}_x$  mixing ratios in 4 different stages at SDZ.



458

**Figure 8.** Mixing ratios of  $\text{SO}_2$  and  $\text{NO}_x$  during different stages as a function of wind direction at SDZ.



459

**Figure 9.** Diurnal variations in mixing depths in four seasons at SDZ.



**Table 1.** Statistics in the hourly mean of SO<sub>2</sub> and NO<sub>x</sub> mixing ratios at SDZ.

	NO (ppb)	NO <sub>2</sub> (ppb)	NO <sub>x</sub> (ppb)	SO <sub>2</sub> (ppb)
Mean	1.10	13.08	14.18	5.71
Standard deviation	2.58	10.89	12.36	8.44
Median	0.33	9.98	10.59	2.45
Maximum	83.34	124.41	147.58	100.34
Minimum	0.01	0.01	0.14	0.01
Count number	104923	104923	104923	105374

460

**Table 2.** NO<sub>x</sub> and SO<sub>2</sub> levels in the atmospheric background stations in China.

Site	Time	NO <sub>x</sub> (ppb)	SO <sub>2</sub> (ppb)	References
SDZ (North China)	2005.1–2017.5	14.2 ± 12.4	5.7 ± 8.4	This study
Linan (Yangtze River Delta)	2005.8–2006.7	–	11.1 ± 10.6	(Qi et al., 2012)
	2006.1–2016.12	13.6 ± 1.2	7.0 ± 4.2	(Yin et al., 2021)
Wuyishan (East China)	2011.3–2012.2	2.70	1.48	(Su et al., 2013)
Dinghushan (South China)	2009.1–2010.12	13.6	6.5	(Chen, 2012)
Changbaishan (Northeast China)	2009.1–2010.12	4.7	2.1	(Chen, 2012)
Fukang (Northwest China)	2009.1–2010.12	8.3	2.2	(Chen, 2012)
Gonggashan (Southwest China)	2017.1–2017.12	0.90	0.19	(Cheng et al., 2019)
Jinsha (Central China)	2006.6–2007.7	5.6 ± 5.5	2.8 ± 5.5	(Lin et al., 2011)

461

**Table 3.** Trends of the hourly mean of the three sectors with the highest SO<sub>2</sub> level, the hourly mean of the three sectors with the lowest SO<sub>2</sub> level and their difference.

	Highest SO <sub>2</sub> values (ppb)	Lowest SO <sub>2</sub> values (ppb)	Difference (ppb)
	W–WSW–SW–SSW sectors	NNW–N–NNE–NE sectors	
Y2005–2008	11.18	3.96	7.23
Y2009–2012	8.12	3.20	4.91
Y2013–2014	7.36	2.35	5.01
Y2015–2017	3.95	1.48	2.48

462